Application of LBM in Simulation of Flow in Simple Micro-Geometries and Micro Porous Media

E. Shirani and S. Jafari
Department of Mechanical Engineering, Isfahan University of Technology, Isfahan, Iran

Isothermal gas flow is simulated in micro-Couette, micro-channel and micro porous media using the lattice Boltzmann model (LBM). To consider compressibility and rarefaction effects, two relaxation time models related to Knudsen number *Kn* and local density are used. Diffuse-scattering boundary condition (DSBC) and a combination of bounce back and specular boundary conditions are used to obtain slip velocity at the wall. For micro-Couette flow, the slip velocity and the slip length as a function of *Kn* are calculated and compared with that of MD, DSMC and Maxwell theorem. For micro-Couette, the velocity profile along with the slip velocity for different values of *Kn* and the slip length as a function of Knudson number are studied. It is shown that the flow structures are changed by changing the values of *Kn*. The nonlinear pressure drop and the velocity distribution along the streamwise direction in the micro-channel flow are obtained and compared with available data, which resulted in good agreement. The Knudsen minimum phenomenon is successfully predicted within the LBM framework. Finally, gas flow characteristics in micro porous media for different *Kn* numbers, porosity and inlet to outlet pressure ratio are studied. The effects of compressibility and rarefaction are considered.

1. Introduction

Micro-electronic-mechanical-systems (MEMS) are a rapidly emerging technology in which micron-scaled devices are constructed using microelectronic fabrication techniques. Many different devices are under development, ranging from channels for integrated cooling of electronic circuits, flow sensors, and valves for gas pressure regulation, to complex systems consisting of channels, pumps, valves, sensors and other components, all integrated on a single module or as sandwiched modules [1]. In order to design such devices effectively, it is necessary to understand and employ the physical laws governing the flow in small conduits. Because of obvious difficulties associated with testing and validating these devices experimentally, numerical analysis is an alternative for investigating the flow inside micro-channels and other more complex geometries [2].

The Knudsen number *Kn*, which is defined as $Kn = \lambda / H$ and compares the mean free path λ to the smallest flow characteristic length *H*, provides a direct means of validating the continuum approach. Fig. 1 describes different regimes of fluid flow depending on the Knudsen number. For $Kn > 10$, the system can be considered to be a free molecular flow. A flow is considered a continuum for $Kn < 0.001$. The intermediate values of *Kn*, for $0.1 < Kn < 10$, are associated with a transition flow regime, while those within the range of $0.001 < Kn < 0.1$ represent a slip flow regime. The Navier–Stokes equations may be applied to flows within the slip regime or marginally transitional if the first-order or higher-order velocity slip boundary conditions are employed at the wall. For flows in the high transition or free molecular regimes, it requires either a direct solution of the full Boltzmann equation, or particle-based methods such as molecular dynamics (MD) [3] or a gas dynamic model such as the direct simulation Monte Carlo (DSMC) [4].

In the last decade or so, the lattice Boltzmann model (LBM) which is also called lattice Boltzmann equation or Boltzmann cellular automata in the literature, has emerged as a new and effective numerical approach of computational fluid dynamics and achieved considerable success in simulating fluid flows and associated transport phenomena. The lattice Boltzmann model is based on microscopic models and mesoscopic kinetic equations. The LBM constructs simplified kinetic models that incorporate the essential physics of microscopic or mesoscopic processes so that the macroscopic averaged properties obey the desired macroscopic equations. In the LBM, a simplified version of the kinetic equation is used rather than solving complicated kinetic equations such as the full Boltzmann equation. It has the advantage of implementation of fully parallel algorithms.

* Corresponding author: eshirani@cc.iut.ac.ir

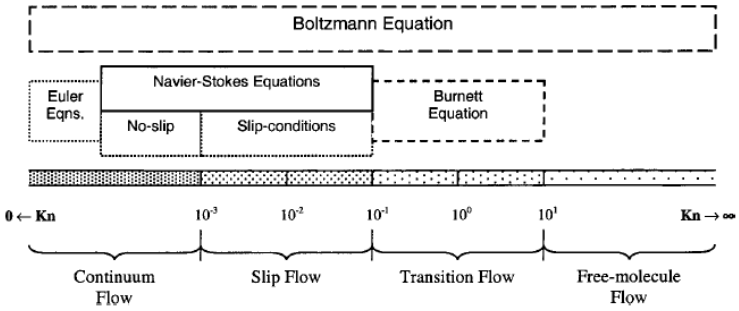

FIG. 1. Knudsen number regimes.

The LBM simulates fluid flows by tracking the evolution of single-particle distribution, and computationally it is a stable, accurate and efficient method. The LBM originated from lattice gas (LG) automata. It can also be viewed as a special finite difference scheme for the kinetic equation of the discrete-velocity distribution function. The LBM encompasses a lattice, an equilibrium distribution and a kinetic equation called, the lattice Boltzmann equation (LBE). The LBM was first introduced by McNamara and Zanetti [5] and it requires much less computational effort than the MD and DSMC. In fact, unlike MD and DSMC methods, the number of particles distributed in the computational field in the LBM is not related to the number of molecules and it is many orders of magnitude less. A simple linearized version of the collision operator, which makes use of a relaxation time τ towards the local equilibrium using a single time relaxation, is the Bhatnagar-Gross-Krook (BGK) collision operator (Bhatnagar *et al.* [6]) and has been independently suggested by several authors (Qian [7], Chen *et al.* [8]). The LBM can be used to simulate flows with a wide range of Knudsen numbers and especially for flows with high *Kn*, where the flow regimes are slip and transition flows. The method is particularly useful in applications involving interfacial dynamics, multiphase and multi-component fluid flows and flows with complex geometries such as flow in porous media [9-11]. The method is also used to simulate turbulent flows (Martinez *et al.* [12] and flows with moderate heat transfer [13-20].

The LBM has three important and distinct features compared to the other numerical methods: The convection operator (or streaming process) of the LBM in phase space (or velocity space) is linear, the incompressible Navier-Stokes (NS) equations can be obtained in the nearly incompressible limit of the LBM and the LBM utilizes a minimal set of velocities in phase space.

To obtain no-slip velocity conditions at the wall, one of the simplest ways is to use the first order method called the bounce-back scheme (Wolfram [21], Lavallee *et al.* [22]). By using this scheme, when a particle distribution streams to a wall node, the particle distribution scatters back to the node it came from. More higher order no-slip boundary conditions were introduced by He *et al.* [23], Skordos [24], Noble *et al.* [25], Inamuro *et al.* [26], Maier *et al.* [27], Zou and He [28], Ziegler [29], Zou *et al.* [30], He *et al.* [23] and Chen *et al.* [31].

For $Kn > 0.001$, the no-slip conditions at the walls do not hold. Because the LBE method is a particle-based method like the direct simulation of Monte Carlo (DSMC) method [4], it is applicable to slip flows. Specular boundary conditions produce free slip conditions at the wall. That is, by using this condition, when a particle distribution streams to a wall node, the particle distribution scatters back in such a way that its velocity component parallel to the wall does not change and its velocity component normal to the wall changes its sign. In reality, the slip velocity is somewhat between no-slip and free-slip conditions. So a combination of bounce back and specular conditions is used to obtain accurate slip-velocity at the wall. This idea was used by Tao [32] and Zhang *et al.* [33]. Another boundary condition which is introduced for velocity slip condition is diffuse-scattering boundary condition (DSBC) (Chew [34]). We will examine both conditions in this work.

The relaxation time τ, which is a typical time scale associated with collisional relaxation to the local equilibrium, appears in the BGK model for a collision operator. In principle, τ is a complicated function of the distribution function *f*. The drastic

simplification associated with the BGK operator is the assumption of a constant value for the relaxation time scale. Constant relaxation time eliminates the compressibility effects which is important for flows with high *Kn*. In order to allow compressibility effects, Lim *et al*. [35] related τ with *Kn*, namely $\tau = Kn\, H / \delta x$, where δx is the computational grid length. Nie *et al*. [36] related the non-dimensional relaxation time τ to *Kn* and the fluid density ρ as $Kn = a(\tau - 0.5)/(\rho H)$, where *H* is the channel height. The factor 0.5 stems from the explicit treatment of the collision term and *a* is chosen to best match the simulated mass flow rate with experiments. This model allows using variable channel width as well as taking into consideration the compressibility effects. Also Tao *et al.* [32] related relaxation time to Knudsen number and local density.

The lattice Boltzmann simulation of the two-dimensional driven cavity by Hou *et al.* [37] covered a wide range of Reynolds numbers from 10 to 10,000 using a 2562 lattice. Two-dimensional cavity flow was also studied by Miller [38].

Nie *et al.* [36] used the LBE method to simulate two-dimensional micro-channel and micro-cavity flows. They employed the half-way bounce back rule at the surface. Lim *et al.* [35] used the specular bounce-back rule and the extrapolation scheme to produce slip effects, and compared their results of two-dimensional channel flows with the experimental data as well as Arkilic's analytical solution [39]. Zhang *et al.* [33] implemented the tangential momentum accommodation coefficient to describe the gas–surface interactions in a LBE-D2Q9. Their boundary conditions work in a spirit similar to the combination of the bounce back rule and specular reflection. Tao *et al.* [32] studied gas flow in micro-channels. They captured suitable slip velocity in wall using combination of bounce back and specular boundary conditions.

Arkilic *et al.* [39] investigated two-dimensional gas micro-channel flows both experimentally and analytically using the Navier -Stokes equations with a first-order slip boundary condition. Chen *et al.* [40] numerically solved the two-dimensional, compressible Navier-Stokes equations along with a first-order slip-velocity boundary condition for gaseous flow in a micro-channel. We compare our LBM results with the results obtained by the above mentioned references.

The aim of the present work is to use lattice Boltzmann methods to simulate gas flow in two-dimensional micro-geometries, to examine the different boundary conditions and relaxation times, to obtain and compare the slip-velocities at different conditions and with different Knudsen numbers, to analyze the effects of compressibility and rarefaction, and to obtain the Knudsen minimum phenomenon using the LBM. We are also interested in the behavior of models when they are used for micro-scale porous media.

2. Lattice Boltzmann method

The kinetic evolution of the lattice Boltzmann equation with the BGK collision approximation is [10]

$$f_i(x + c_i \Delta t, t + \Delta t) = f_i(x,t) - \frac{1}{\tau}\left[f_i(x,t) - f_i^{eq}(x,t)\right], \tag{1}$$

where τ is the dimensionless relaxation time. Eq. (1) is a discrete finite difference equation, which is second order accurate with respect to space and time. For D2Q9 lattice model, that is, for two-dimensional problem with nine velocity model (see Fig. 2) the discrete velocities are given by:

for $i = 0$:

$$c_i = 0$$

for $i = 1, 2, 3, 4$:

$$c_i = (\cos(i-1)\pi/2, \sin(i-1)\pi/2)c$$

for $i = 5, 6, 7, 8$

$$c_i = \sqrt{2}(\cos[(i-5)\pi/2 + \pi/4], \sin[(i-5)\pi/2 + \pi/4])c$$

The streaming speed c is defined as $\Delta x / \Delta t$, where Δx and Δt are the lattice spacing and time step, respectively.

The equilibrium distribution function f_i^{eq} for the D2Q9 model is

$$f_i^{eq} = w_i \rho \left[1 + 3(c_i.U)/c^2 + 4.5(c_i.U)^2/c^4 - 1.5U^2/c^2\right] \tag{2}$$

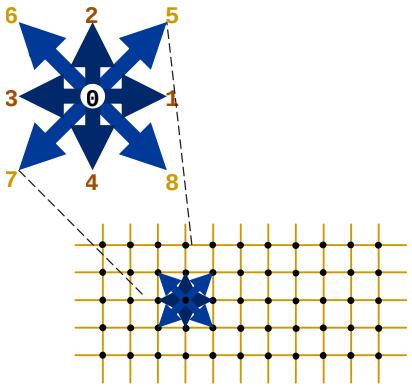

FIG. 2. D2Q9 Model.

where $w_0 = 4/9$ and $w_i = 1/9$ for i = 1,2,3,4, and $w_i = 1/36$ for $i = 5,6,7,8$. The macroscopic variables for the fluid mass density, fluid momentum, and pressure are defined by $\rho = \sum_{i=0}^{9} f_i$, $\rho U = \sum_{i=0}^{9} c_i f_i$ and $P = \rho c^2 / 3$. The term τ in Eq. (1) is replaced by τ' to take into account the gas compressibility [12].

$$\tau' = \frac{1}{2} + \frac{\rho_{ref}}{\rho}\left(\tau - \frac{1}{2}\right), \qquad (3)$$

where ρ_{ref} is a referenced density and τ is linked with the channel outlet Knudsen number Kn_o via the following equation:

$$\tau = \frac{\rho_o N_y Kn_o}{\rho_{ref}\sqrt{\pi/6}} + \frac{1}{2} \qquad (4)$$

where ρ_o is the outlet gas density and N_y is the characteristic lattice number.

The slip velocities on all the solid block surfaces and the plate wall boundaries are implemented by combining the bounce-back with the specular reflection. We define a reflection coefficient r_b as the proportion of bounce-back reflections in the interactions with the wall and $1 - r_b$ represent the specular reflections proportion. We used $r_b = 0.7$, as compared to results from Arkilics' model [39], to best capture the slip-velocity on the solid-gas wall implying that more fluid particles will be reflected in the backward direction than the forward direction.

3. Results and discussion

Numerical simulation for different *Kn* numbers and three flow configurations: flow in a micro-Couette, micro-channel and in a porous media, are presented.

3.1 Micro-Couette

Flow between two parallel plates, when the upper plate moves at a constant velocity and the lower plate is stationary, is studied for various Knudson numbers. Figure 3 shows the velocity profile of the gas between the two plates for four different *Kn* numbers, 0.001, 0.02, 0.1, and 0.5. As expected, the slip velocity increases with increasing *Kn*, but the velocity profile remains linear and symmetric. The slip velocity is negligible for *Kn< 0,01*. To examine the validity of the method as well as the model for boundary conditions, we have calculated the slip length, $\xi = U_s / \dot{\gamma}_w$, where U_s is the slip velocity and $\dot{\gamma}_w = \partial u_w / \partial y$ is the strain rate. The results shown in Fig. 4 were plotted against the *Kn* number and compared with that of MD, DSMC and Maxwell theorem [41-42] resulting in an excellent agreement as shown in the figure below.

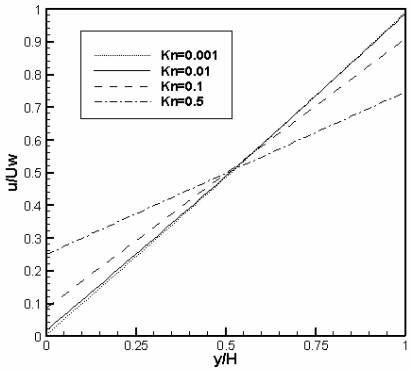

FIG. 3. Velocity profile for different Kn for Couette flow.

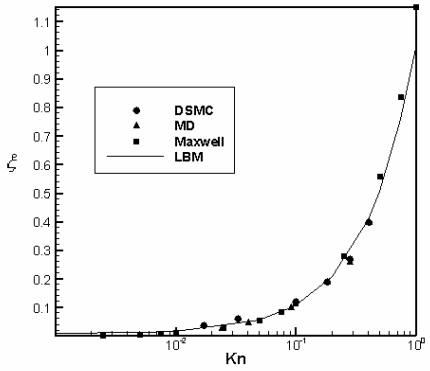

FIG. 4. Slip length as a function of *Kn* for Couette flow.

3.2 Micro-channel

Flow in a micro-channel is simulated using the LBM. The height of the channel is fixed at H = 1.2 μ and the length is kept constant at $L = 100H$. The working fluids are carbon dioxide (CO2), nitrogen (N2), hydrogen (H2), and helium (He). Their corresponding Knudsen numbers at the channel outlet Kn_o are 0.0236, 0.055, 0.1, and 0.16, respectively. Deviations of pressure from linear pressure drop (i.e., corresponding to incompressible fully developed laminar flow) for different inlet pressures with the same outlet Knudsen number are shown in Fig. 5. Here the vertical coordinate of the plot is expressed as $\overline{P} = (P - P_{in})/P_o$. As can be seen, for the same outlet Knudsen number $Kn_o = 0.055$, the increase in the inlet pressure (i.e., an increase in compressibility within the channel) results in a larger deviation from the linear pressure distribution as it is expected in an incompressible channel flow. Furthermore, the location of maximum deviation from linear pressure distribution moves toward the channel exit as the inlet pressure increases. In this figure, the Arkilics' analytical solutions are also shown. The agreement is excellent and the locations of the maximum deviation from linear pressure distribution are calculated accurately. The effects of different outlet Knudsen number when the inlet to outlet pressure ratio is fixed are shown in Fig. 6. As Kn_o increases, stronger rarefaction effects are observed which corresponds to smaller deviation from the linear pressure distribution. This means that the rarefaction effects tend to decrease the pressure distribution deviation caused by the compressibility effect. Thus, the compressibility effect and the rarefaction effect have contradicting influence on the pressure distribution. The distribution of the pressure along the channel is somewhat a balance between these two effects. The variation of slip-velocity along the length of the wall is presented in Fig. 7. Due to the pressure drop along the channel, the local Knudsen number increases, resulting in an increase in the slip-velocity in the streamwise direction. In our simulation results, the magnitude and variation trend of the slip-velocity agree well with Arkilics' model when a combination of bounce back and specular reflection with $r_b = 0.7$ is used at the wall boundary condition. Figure 8 shows the average velocity variations along the streamwise direction. The predicted results of the present study and those of Arkilics' are too close to be plotted as separated curves. Figure 9 shows the ratio of the flow rate at micro-channel to the flow rate of conventional fully developed channel flows as a function of Knudson number. It can be seen that by increasing the Knudson number, the flow rate first decreases and then it increases. This phenomenon was first observed by Knudson and is now called Knudson minimum. It is due to the fact that at the lower Knudson numbers, the compressibility effect is dominant and thus by increasing the Knudson number, the pressure drop is increased and it resists the flow in the channel. But at higher Knudson numbers, the rarefaction effect is dominant and causes the flow rate increase by increasing the Knudson number.

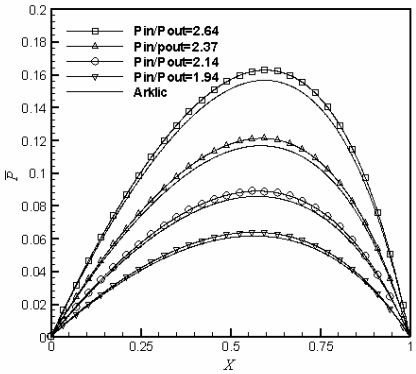

FIG. 5. Nonlinearity of pressure along the channel for *Kn =0.055*and different P_{in}/P_{out}.

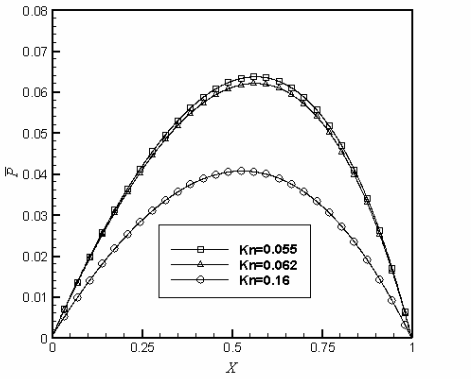

FIG. 6. Nonlinearity of pressure along the channel for P_{in}/P_{out} = 1.94 and different Kn.

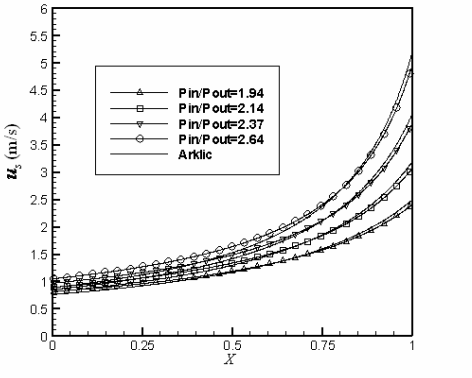

FIG. 7. Slip-velocity distributions along the wall for *Kn* =0.055.

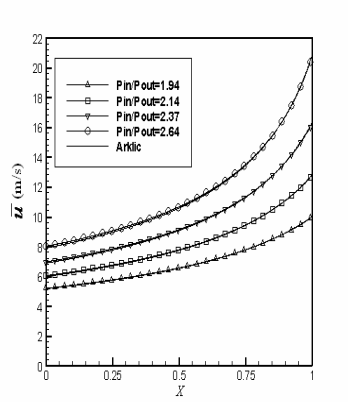

FIG. 8. Average gas velocity along the channel for *Kn =0.055*.

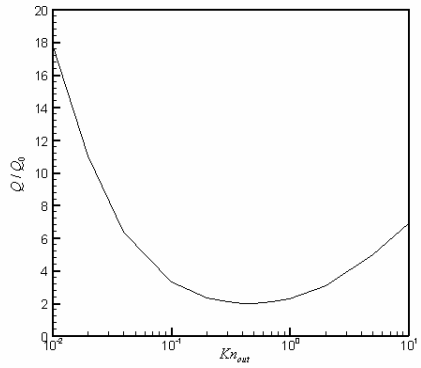

FIG. 9. Mass flow rate in channel for P_{in}/P_{out} = 1.43 as a function of *Kn*.

3.3 Two-dimensional micro-scale porous media flow

In order to study the flow in porous media, two-dimensional disordered solid blocks are packed between two parallel plates (see Figs. 10). Porosity ε represents the fraction void volume in the porous structure and is defined as $\varepsilon = (V - V_s)/V$, where V is the total volume and V_s is the volume of the solid blocks. The height of the simulated channels is $H = 1.2\mu$ and the ratio of the channel length L to the height H is 2. Isothermal gaseous flows in such micro scale porous structures are simulated using the lattice Boltzmann method. The calculated results of velocity vectors for different values of Knudsen number at inlet to outlet pressure ratio, P_{in} / P_{out} = 1.1, are shown in Figs. 10. At higher values of Knudsen number, the slip velocities on the bottom and top plates are much larger than those at the lower Knudsen number. Conversely, the velocities away from the plates are lower. The volume flow rates per unit area as a function of the inlet to outlet pressure difference, for four values of porosity: $\varepsilon = 0.711,\ 0.765,\ 0.802, 0.856$ and for two different outlet Knudson numbers, are shown in Figs. 11a and 11b, respectively. The Knudsen number has significant influence on the flow rate. The figures shows that for the same pressure gradient, the volume flow rate increases with the increase of Knudsen number, implying a reduction in friction drags on the walls and blocks. The flow rate increases steeply with increasing porosity. However, for structures with relatively small porosity, the flow rate is effected to a

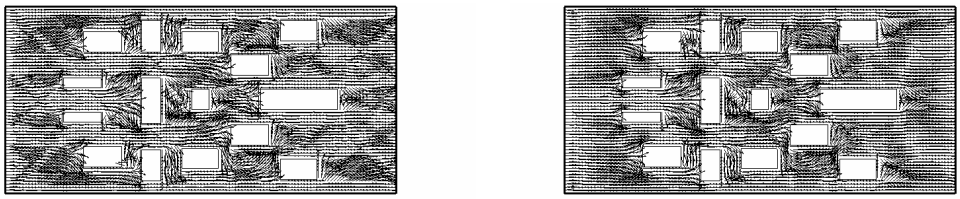

(a) Kn_o = 0.055 (b) Kn_o = 0.16

FIG. 10. Velocity vectors for flow in the porous structure, ε = 0.765 and P_{in} / P_{out} = 1.1.

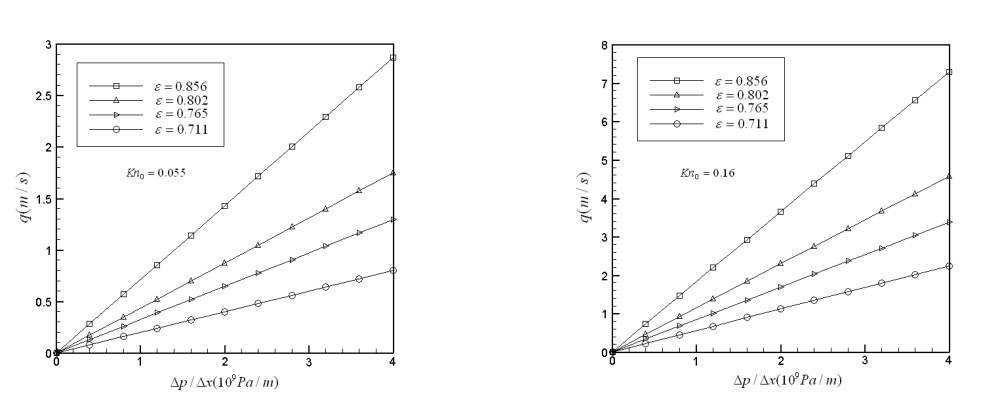

(a) Kn_o = 0.055 (b) Kn_o = 0.16

FIG. 11. Volume flow rate as a function of the pressure gradient for various ε and *Kn*.

lesser degree than those having higher levels of porosity. The results obtained through simulation using the presented LBM method are qualitatively consistent with the experimental data [43]. Finally, we compare the calculated results of pressure drops with the following empirical equations based on experimental data, the Ergun correlation [44] and the Carman-Kozeny correlation [45] as shown in Fig. 12. First, we tried to determine the value of the equivalent diameter of the body D_p for the porous structure of ε = 0.765 by comparing the calculated pressure drop with the Carman-Kozeny equation and the Ergun equation. We simulated the flow for Kn_o = 0.001 because it can be considered as a continuum flow. Comparing the calculated results with the above mentioned two empirical equations, we found good agreement when D_p = 0.16μm. The calculated dimension-less pressure drops are lower than the ones obtained by the Ergun equation for the other four Knudsen numbers at lower Reynolds numbers as indicated in Fig. 12. To fit the data for different Knudsen numbers with a single straight line, we scale up the pressure drop by multiplying it by $(1+AK\overline{n})$ as shown in Fig. 13. Here $K\overline{n}$ is the mean Knudsen number of the inlet and outlet and *A* is a constant. The data are in good agreement with the Ergun equation and the Carman-Kozeny equation if *A* is set to be 70.

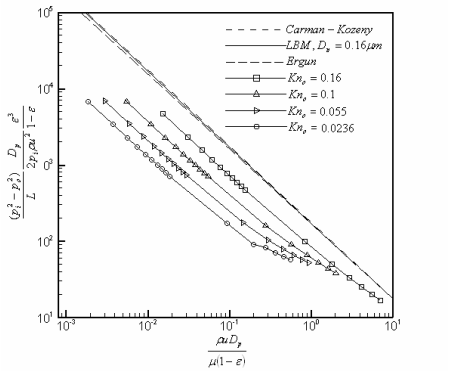

FIG. 12. Pressure drops considering compressibility versus *Re* for ε = 0.765.

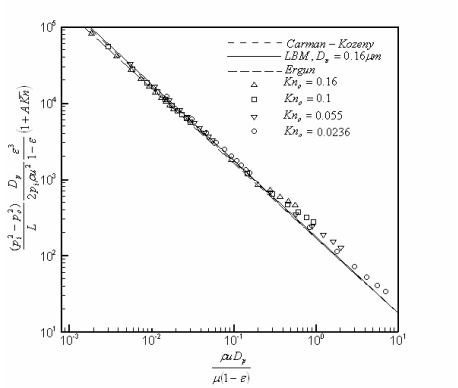

FIG. 13. Pressure drops considering compressibility versus *Re* for $\varepsilon = 0.765$.

4. Conclusion

The lattice Boltzmann method (LBM) is used to study gas flow in micro-geometries. It was shown that the slip velocity obtained in micro-Couette flow at different values of Knudson number is very accurate and similar to that of very expensive calculations of MD and DSMC methods. Characteristics in the two-dimensional micro-channel flow including slip-velocity, nonlinear pressure drop and average velocity along the streamwise direction were all compared with the available data resulting in a good agreement. This shows that the lattice Boltzmann method is a promising approach for simulating the flow in micro-channels. The influence of gas rarefaction in porous media is considered. The transport characteristics in relatively simple porous structures are studied with the presented LBM method. Considering the compressibility and the rarefaction, a model for the pressure drop is presented based on the Ergun equation and the Carman-Kozeny equation.

References

[1] C. M. Ho, Ann. Rev. Fluid Mech. **30**, 579 (1998).
[2] M. Gad-El-Hak, J. Fluids Eng. **12**, 5 (1999).
[3] G.A. Bird, *Molecular Gas Dynamic and the Direct Simulation of Gas Flow*, (Oxford University Press, 1994).
[4] E. S. Oran, Ann. Rev. Fluid Mech. **30**, 403 (1998).
[5] G. R. McNamara, and G. Zanetti, Phys. Rev. Lett. **61**, 2332 (1988).
[6] P. L. Bhatnagar, E. P. Gross, and M. Krook, Phys. Rev. **94**, 511 (1954).
[7] Y. H. Qian, "Lattice gas and lattice kinetic theory applied to the Navier-Stokes equations", PhD thesis, Universit`e Pierreet Marie Curie, Paris (1990).
[8] S. Chen, H. D. Chen, D. Martinez, and W. Matthaeus, Phys. Rev. Lett. **67**, 3776 (1991).
[9] A. Wolf-Gladrow, *Lattice-gas Cellular Automata and Lattice Boltzmann Method*, (Springer, 2002).
[10] S. Chen, Ann. Rev. Fluid Mech., **30**, 329 (1998).
[11] S. Succi, *The Lattice Boltzmann Equation: For Fluid Dynamic and Beyond Series Numerical Mathematics and Scientific Computation*, (Oxford University Press, 2001).
[12] D. O. Martinez, W. H. Matthaeus, S. Chen, and D. C. Montgomery, Phys. Fluids **6**, 1285 (1994).
[13] X. D. Niu, C. Shu, and Y. T. Chew, Computers & Fluids **36(2)**, 273 (2007).
[14] C. Chen, T. S. Yen, and Y. T. Yang, Int. J. of Heat and Mass Transfer, **49**, 1195 (2006).
[15] C. Chen, T. S. Yen, and Y. T. Yang, Int. J. of Thermal Sciences **45**, 982 (2006).
[16] X. He, S. Chen, and G. Doolen, J. Comp. Phys. **146**, 282 (1998).
[17] A. D'Orazio, and S. Succi, Future Generation Computer Systems, **20**, 935 (2004).
[18] Y. Peng, C. Shu, and Y. T. Chew, J. of Comp. Phys. **193**, 260 (2003).
[19] O. Zou, and X. He, http://arxiv.org/abs/comp-gas/9611001 V1.
[20] Y. T. Chew, X. D. Niu, and C. Shu, Proc. CHT-04, Norway (2004).
[21] S. Wolfram, J. Stat. Phys. **45**, 471 (1986).
[22] P. Lavall´ee, J. P. Boon, and A. Noullez, Boundaries in lattice gas flows, Physica D **47**, 233 (1991).
[23] X. He, Q. Zou, L-S Luo, and M. Dembo, J. Stat. Phys. **87**, 115 (1997).
[24] P. A. Skordos, Phys. Rev. E **48**, 4823 (1993).
[25] D. R. Noble, S. Chen, J. G. Georgiadis, and R. O. Buckius, Phys. Fluids **7**, 203 (1995).
[26] T. Inamuro, and B. Sturtevant, Phys. Fluids **2**, 2196 (1990).
[27] R. S. Maier, R. S. Bernard, and D. W. Grunau, Phys. Fluids **8**, 1788 (1996).
[28] Q. Zou, and X. He, Phys. Fluids. **9**, 1591 (1997).

[29] D. P. Ziegler, J. Stat. Phys. **71**, 1171 (1993).
[30] Q. Zou, S. Hou, and G.D. Doolen, J. Stat. Phys. **81**, 319 (1995).
[31] S. Chen, D. Martinez, and R. Mei, Phys. Fluids **8**, 2527 (1996).
[32] W. Q. Tao, Int. J. of Mod. Phys. C, **15**, 335 (2004).
[33] Y. H. Zhang, J. of Stat. Phys. **121**, 257 (2005).
[34] X. Niu, D. C. Shu, and Y. T. Chew, Europhys. Lett. **67**, 600 (2004).
[35] C. Y. Lim, J. Phys. Fluids, **14**, 2299 (2002).
[36] X. Nie, J. Stat. Phys. **107**, 279 (2002).
[37] S. Hou, "Lattice Boltzmann method for incompressible viscous flow", PhD thesis, Kansas State Univ., Manhattan, Kansas (1995).
[38] W. Miller, Phys. Rev. E **51**, 3659 (1995).
[39] E. B. Arklic, J. Micro-electro-mech. System **6**, 167 (1997).
[40] C. S. Chen, Numerical Heat Transfer, Part A, **33**, 749 (1998).
[41] D. L. Morris, L. Hannon, and A. L. Garcia, Phys. Rev. A **46(8)**, 5279 (1992).
[42] D. R. Willis, Phys Fluids. **5**, 127 (1962).
[43] S. Roy, J. of Appl. Phys. **93**, 4870 (2003).
[44] S. Ergun, Chemical Engineering Progress **48**, 89 (1952).
[45] A. E. Scheidrgger, *The Physics of Flow Through Porous Media* (University of Toronto Press, 1972).

Received: 14 August, 2007
Accepted: 23 August, 2007